

Electronic Supplementary Information for

Fluorescent Enhancement of Perovskite Nanocrystals by Photonic Crystals

*Songyan Yuan,^a Xinran Zhang,^a Wenjing Cao,^b Yuhang Sheng,^a Cihui Liu,^{*a} Liyan Yu,^c Lifeng Dong,^c Yunsong Di,^a Zihui Chen^{*b} and Zhixing Gan,^{*a,c}*

^a Center for Future Optoelectronic Functional Materials, School of Computer and Electronic Information/School of Artificial Intelligence, Nanjing Normal University, Nanjing 210023, China

^b Key Lab of Advanced Transducers and Intelligent Control System, Ministry of Education and Shanxi Province, College of Physics and Optoelectronics, Taiyuan University of Technology, Taiyuan 030024, China

^c College of Materials Science and Engineering, Qingdao University of Science and Technology, Qingdao 266042, P. R. China

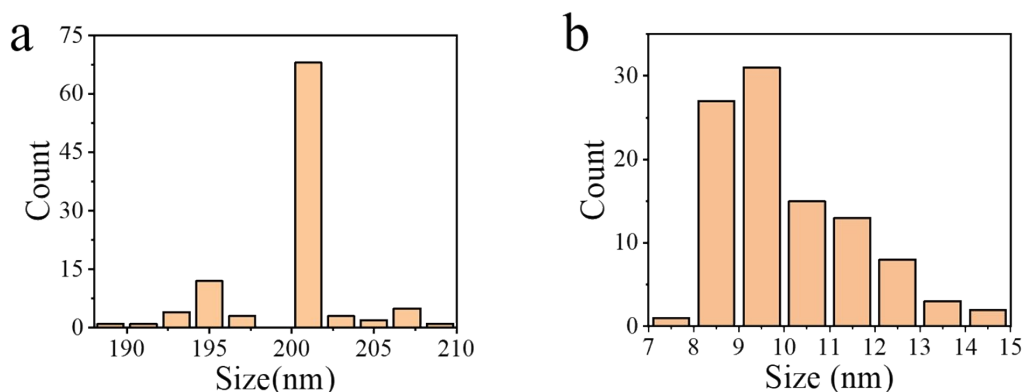


Fig. S1 Size distributions of (a) SiO₂ nanospheres and (b) CsPb(Br_{0.51}Cl_{0.49})₃ PNCs.

Table S1. Analysis of PL decays of PNCs on glass and PCs.

	A_1	$\tau_1(\text{ns})$	A_2	$\tau_2(\text{ns})$	$\tau_{av}(\text{ns})$
PNC on glass	41114.1	1.83	11584.	9.26	6.20
6					
PNC on PCs	46198.8	0.99	2745.0	6.63	2.60

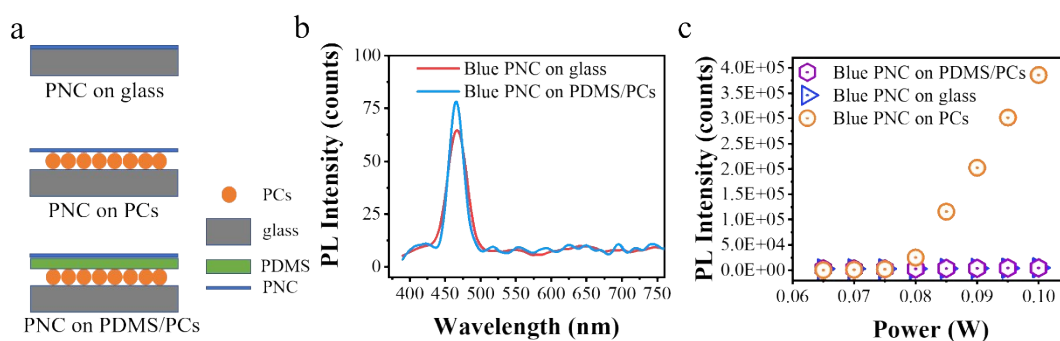


Fig. S2 (a) Schematic diagrams of PNCs on glass, PNCs on PCs, and PNCs on PDMS/PCs. (b) PL spectra of PNCs on glass and PDMS/PCs. (c) Integral PL intensities of PNCs on glass, PNCs on PDMS/PCs, PNCs on PCs versus excitation

powers.

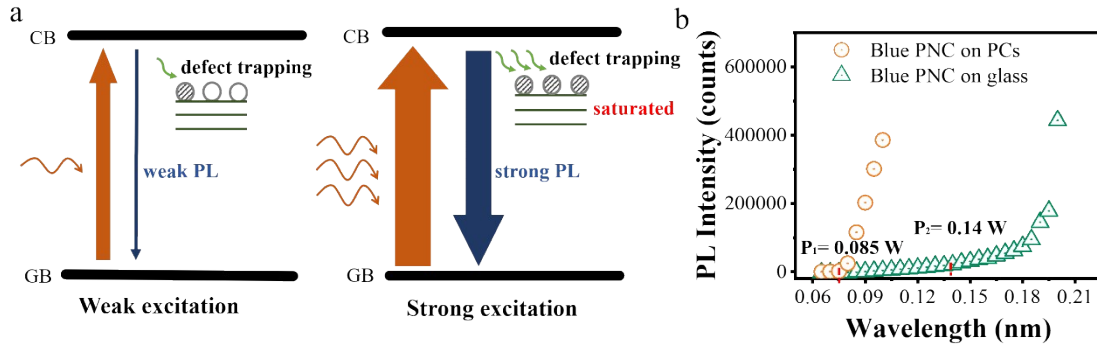


Fig. S3 (a) Schematic diagram of the trap filling effect. (b) Integral PL intensities of blue PNCs on PCs and blue PNCs on glass at different excitation powers.

As illustrated in Figure S3a, if the PNCs are weakly excited, a part of the photogenerated excitons may be trapped by the defect states, leading to a low PL efficiency. Whereas, when the excitation power is high enough, the trap states are gradually saturated. Thus, the PL intensity of perovskites super-linearly increases with the excitation density. The PL intensity of PNCs on glass versus excitation power is shown in Fig. S3c. When the excitation power is higher than 0.14 W, the PL intensity super-linearly increases. Regarding the PNCs on PCs, since the excitation is enhanced by the near field of the PCs, the non-radiative traps of the PNCs are saturated at a lower excitation (0.085 W). The near field of PCs resonates with the excitation light, which is equivalent to enhancing the excitation power.

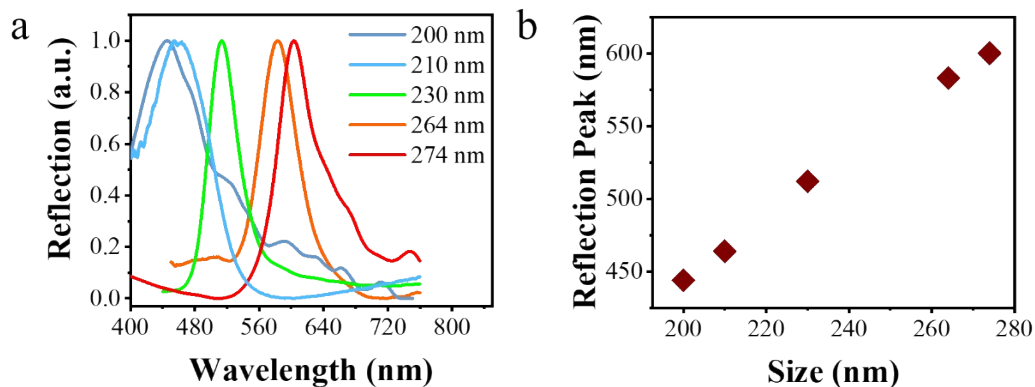


Fig. S4 (a) Reflection spectra of photonic crystals with different SiO₂ sizes. (b) Plots

of the reflection peak positions versus SiO₂ diameters.

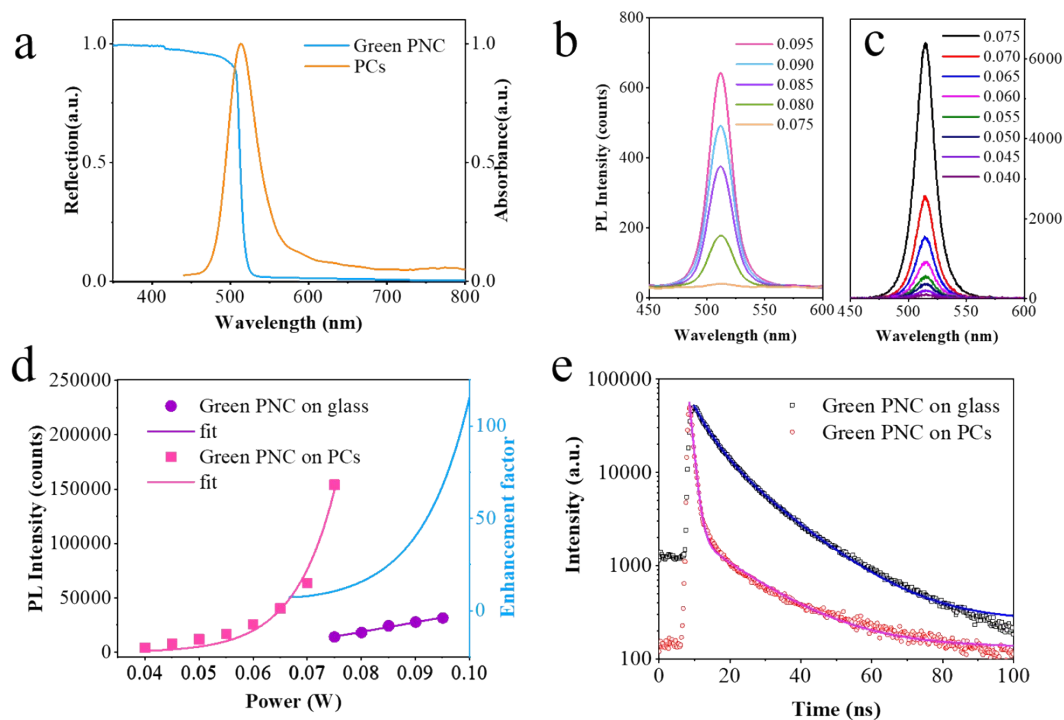


Fig. S5 (a) Normalized absorption spectra of CsPbBr₃ PNCs and reflection spectra of 230 nm-SiO₂ PCs. PL spectra of (b) CsPbBr₃ PNCs on glass and (c) PCs at different excitation powers. (d) Integral PL intensities versus excitation powers and their fitting curves (left longitudinal axis), enhancement factors are calculated from the fitting curves (right longitudinal axis). (e) Time-resolved PL curves of CsPbBr₃ PNCs on glass and PCs after normalization.

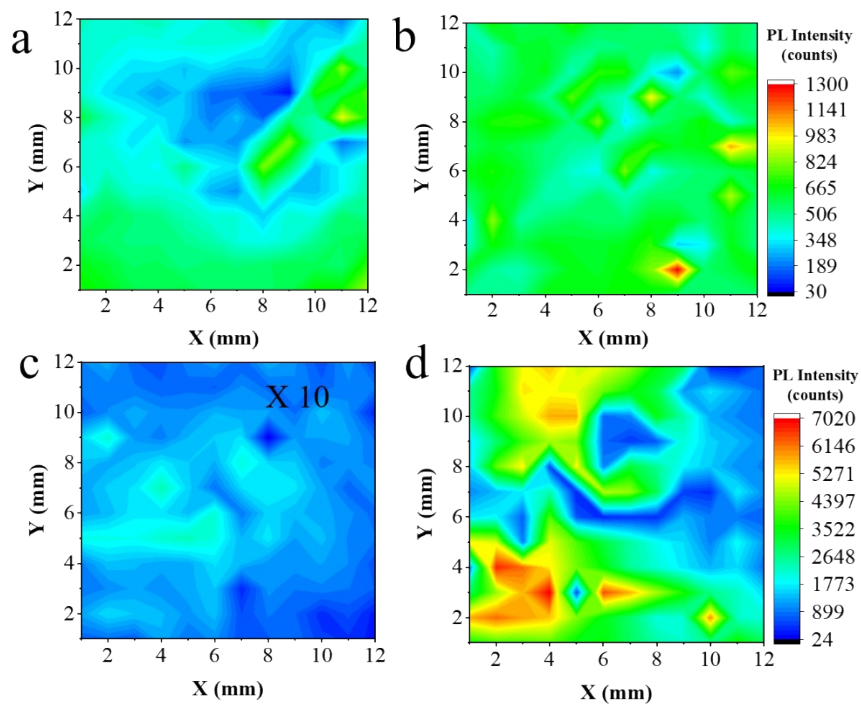


Fig. S6 Two-dimensional PL mappings of (a) CsPbBr₃ PNCs on glass and (b) PCs, (c) CsPb(Br_{0.45}I_{0.55})₃ PNCs on glass and (d) PCs. The PL intensity of CsPbBr₃ PNCs on glass is magnified tenfold in (c).

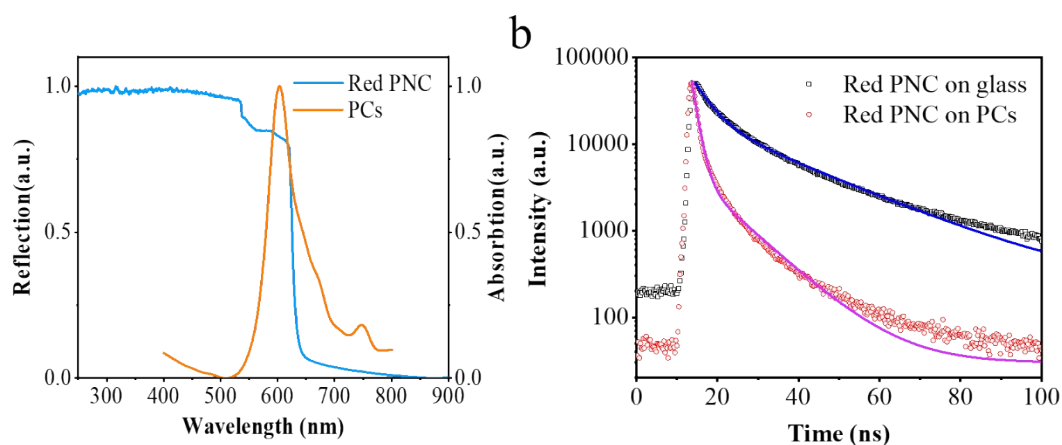


Fig. S7 (a) Normalized absorption spectra of CsPb(Br_{0.45}I_{0.55})₃ PNCs and reflection spectra of 274 nm-SiO₂ PCs. (b) Time-resolved PL curves of CsPb(Br_{0.45}I_{0.55})₃ PNCs on glass and PCs after normalization.

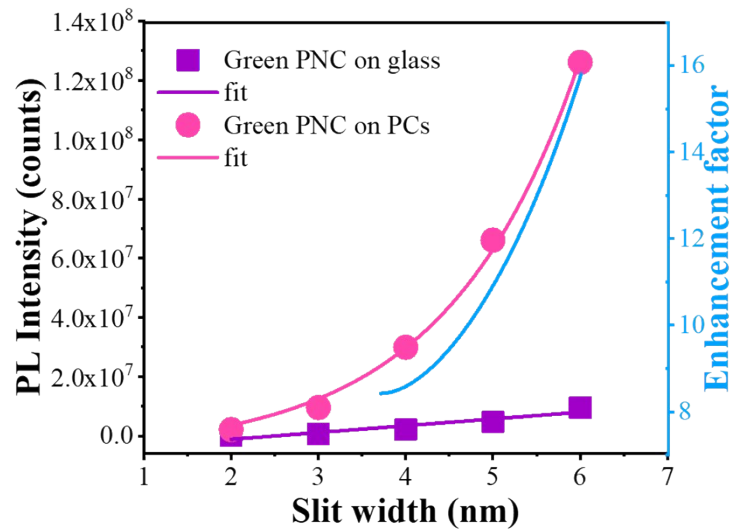


Fig. S8 Integral PL intensities versus excitation powers when the excitation source is a 365 nm monochromatic light from xenon lamp (left longitudinal axis), enhancement factors are calculated from the fitting curves (right longitudinal axis). The excitation slit width is changed from 2 to 6 to control the excitation power.

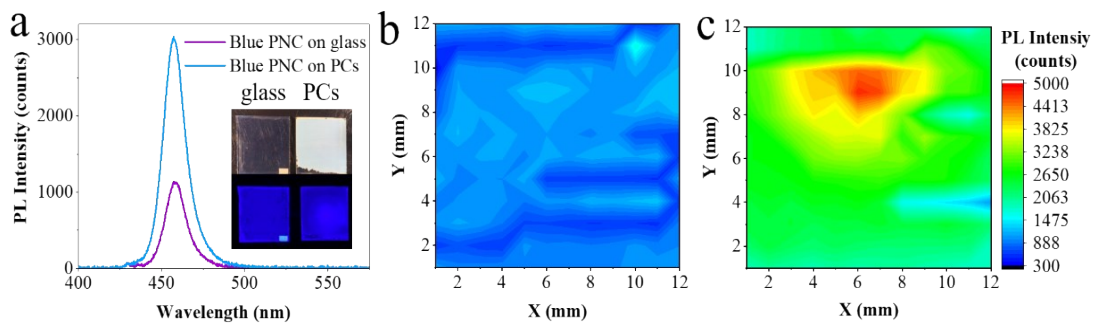


Fig. S9 (a) Emission spectra of $\text{CsPb}(\text{Br}_{0.51}\text{Cl}_{0.49})_3$ PNCs on glass and PCs (spin-coating for 1 time) excited at 405 nm. Insets represent the images of samples under sunlight (above) and ultraviolet light (below). Two-dimensional PL mappings of (b) $\text{CsPb}(\text{Br}_{0.51}\text{Cl}_{0.49})_3$ PNCs on glass and (c) PCs.

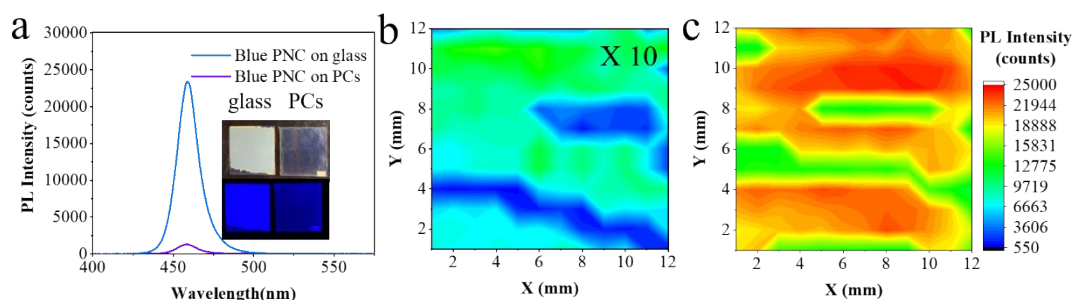


Fig. S10 (a) Emission spectra of $\text{CsPb}(\text{Br}_{0.51}\text{Cl}_{0.49})_3$ PNCs on glass and PCs (spin-coating for 5 times) excited at 405 nm. Insets represent the images of samples under sunlight (above) and ultraviolet light (below). Two-dimensional PL mappings of (b) $\text{CsPb}(\text{Br}_{0.51}\text{Cl}_{0.49})_3$ PNCs on glass and (c) PCs. The intensity of (b) is magnified tenfold.

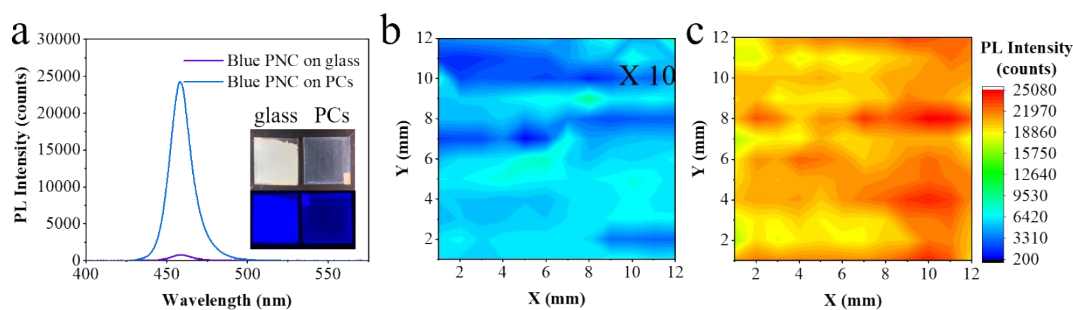


Fig. S11 (a) Emission spectra of $\text{CsPb}(\text{Br}_{0.51}\text{Cl}_{0.49})_3$ PNCs on glass and PCs (spin-coating for 10 times) excited at 405 nm. Insets represent the images of samples under sunlight (above) and ultraviolet light (below). Two-dimensional PL mappings of (b) $\text{CsPb}(\text{Br}_{0.51}\text{Cl}_{0.49})_3$ PNCs on glass and (c) PCs. The intensity of (b) is magnified tenfold.

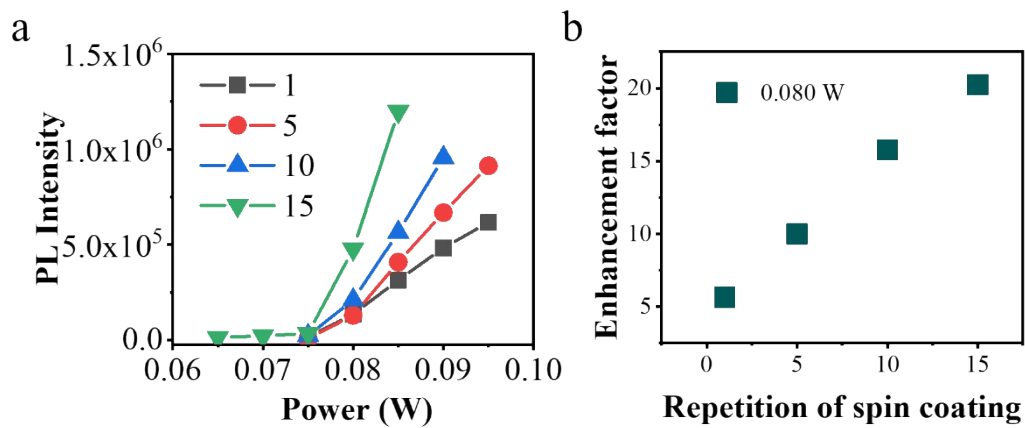


Fig. S12 (a) Comparison of blue PL intensities of $\text{CsPb}(\text{Br}_{0.51}\text{Cl}_{0.49})_3$ PNCs on PCs

(spin-coating for 1, 5, 10, and 15 times) under different excitation powers. (b)

Enhancement factors versus spin-coating times at the same excitation power (0.08 W).